PROPERTIES OF INDIUM DOPED CdS THIN FILMS AND THEIR PHOTOVOLTAIC APPLICATION IN CdTe SOLAR CELLS

Y. CHEN, F. WANG, H. XU, S. REN, H. GU, L. WU*, W. WANG, L. FENG
College of Materials Science and Engineering, Sichuan University, Chengdu, China 610064

Cadmium sulfide thin films with different doping concentration of indium were deposited by magnetron sputtering. The effects of indium concentration on the structure, electrical and optical properties of CdS thin films were studied. XRD results show that all In-doped CdS thin films mainly have face-centered cubic structure with preferred orientation in (111) direction. The optical band gap of CdS:In films varied with indium concentration while the average grain size has an opposite dependency on indium. The carrier concentration increased by 1~3 magnitudes with indium concentration. CdTe solar cells based on CdS:In window layer were fabricated to verify the doping effect of indium on CdS thin films. Photo current density-voltage characteristics and EQE spectra suggest that indium can effectively enhance the collection of carriers in depletion area, which leads to improve both V_{oc} and J_{sc}. Indium doped CdS layer coupled with standard CdTe preparation process has yielded up to 15.53% efficiency solar cell on commercialized TCO substrates.

(Received November 25, 2016; Accepted January 3, 2017)

Keywords: Cadmium sulfide, Indium, Doping, Thin films, CdTe solar cells

1. Introduction

Cadmium sulfide (CdS) is one of the most promising photovoltaic materials[1, 2, 3] due to its wide band gap(2.42eV)[4]. CdS film has been widely used as window layers of CdTe and CIGS based solar cells. The CdS thin films used to prepare the CdTe solar cells are mostly n-type semiconductors. CdS mainly exists as hexagonal or cubic phases[5, 6]. The structure of CdS thin films are usually influenced by the deposition method and technology. CdS thin films were reported by groups using a variety of film growth techniques, such as spray pyrolysis[7, 8], thermal evaporation[9, 10], electrochemical deposition[10], electron beam evaporation method[11], close-spaced sublimation[12], magnetron sputtering[13], chemical bath deposition[14] and laser ablation[15].

Currently, the highest efficiency of CdS/CdTe solar cells has already reached 22.1%[16] . In order to improve the efficiency of CdTe solar cells, enhancing carrier concentration of n-type CdS window layer is one of the key points. Un-doped CdS thin films generally have high resistivity and doping is a good way to reduce it. Several trivalent ions such as In^{3+}, Al^{3+}, Ga^{3+} and B^{3+} have been doped into CdS so far[17, 18, 19, 20]. It was found that indium-doped CdS thin films showed lower resistivity and better doping effect than those doped with other elements. CdS:In film was also found to be a very desirable window layer material. M.A.Islam et al.[21]

* Corresponding author: wulily77@163.com

reported the opto-electrical properties of indium doped CdS films by sputtering, but the carrier concentration is only 10^{16}~$10^{17}cm^{-3}$ and they did not apply it to fabricate solar cells.

Indium is a kind of rare element in the Earth. In this paper, we focused on the properties of CdS with low indium concentration（at% <1%）and the effect of CdS:In window layer on performance of CdTe solar cells. The indium doping concentration is controlled by changing the sputtering power of indium target. The optical and electrical properties of CdS:In films have been characterized and some new results which are different from the highly doped CdS:In film[22, 23] were obtained. Based on CdS:In window layers, CdTe solar cells with efficiency over 15% were demonstrated on commercialized TCO substrates.

2. Experiment

2.1. Preparation of CdS:In films

In this research, CdS:In thin films were fabricated by magnetron sputtering on a silica glass substrate at room temperature. The background vacuum was 5×10^{-4} Pa. The CdS and indium targets were used for co-sputtering. CdS thin films with indium atomic concentration from zero to 5% (Undoped, 0.2%, 0.4%, 0.8%, 1%, 3%, and 5%) were prepared by controlling the power of each target. There is a moving baffle between the target and the substrate. The substrate holder was kept rotating so that CdS thin films can be more homogeneous. The sputtering ambient is argon with the flow rate of 50 sccm at 1 Pa. There was no annealing process after the preparation of CdS:In thin films.

CdTe solar cells were fabricated on Pilkington Tec15 FTO substrates. The substrates were experienced polish process before the deposition of CdS layer to obtain low surface roughness. CdS:In(30 nm)/CdS(20 nm) complex window layer was deposited on polished FTO substrate. Both un-doped and In-doped CdS thin films were deposited by magnetron sputtering at room temperature in Ar atmosphere. CdTe absorber layers were deposited by close spaced sublimation (CSS) using 5N (99.999%) purity CdTe powders. The substrate temperature(T_{sub}) and the source temperature(T_{sou}) of CdTe were 540℃ and 620℃, respectively. The typical thickness of CSS-grown CdTe layers was about 6 μm. $CdCl_2$ post treatment was carried out at 385℃ for 35 minutes in N_2+O_2 ambient. After heat treatment, the surface of CdTe films was etched using 0.2% bromine /methanol for 8s. The ZnTe:Cu (70 nm) back contact was deposited by co-evaporation from ZnTe and Cu, followed by annealing process at 276℃ for 5 min in nitrogen ambient. Gold was coated as electrode at last. The contact area was defined by evaporating gold through a metal mask, followed by hand scribing with a razor blade to remove the active region around each Au contact.

2.2. Characterization

The film thickness was measured by a stylus surface profilometer (Ambios XP-2). The concentration of indium was measured by ICP-OES (SPECTRO ARCOS). X-ray diffraction measurement was performed using a DX-2600 X-ray diffractometer (Dandong Fangyuan Instrument Company, China) with Cu Ka radiation and the scan ranged from 10° to 70°. The transmittance spectra of CdS:In thin films on glass substrates were measured using a PerkinElmer Lambda 950 UV−Vis Spectrometer. The Hall measurement system was used to measure the electrical properties such as resistivity, mobility and carrier concentration of CdS:In films. The square resistance of the film was measured by four-probe method. The current−voltage characteristics were measured (by SCT3.0, Zhongsen Xi'an) under simulated AM1.5 sunlight at 100 mW·cm^{-2} irradiation and calibrated using a GaAs reference cell to trace NREL standard. The external quantum efficiency (EQE) was measured using a QEX10 solar cell quantum efficiency measurement system (PV Measurements, Inc.).

3. Results and discussion

3.1. Composition and crystal structure of CdS:In thin films

All CdS and CdS:In films were prepared with 150nm thickness. The measured indium concentration was shown in table 1. The indium concentration is very low, so it's hard to be mesured accurately. But the growing regularity is consistent.

Table 1 Mesured concentration and calculated concentration.

Calculated concentration of indium	Mesured concentration of indium
0.2%	0.07%
0.4%	0.12%
1.00%	0.3%
3%	1.63%
5%	2.88%

The crystal structure of CdS:In thin film was studied by XRD as shown in Fig.1. The results revealed that a strong diffraction peak appeared at 26.6°(2θ) for all CdS films with different indium concentration. Compared with the standard PDF card, we know that this peak is corresponding to (111) crystal face in face-centered cubic phase of CdS film. There is also a small diffraction peak appearing at about 47.8°, which is indexed as (103) crystal face in hexagonal structure of CdS. Indium could not be detected out by XRD due to its low concentration in CdS thin films. Fig. 1 shows that CdS:In films were mainly cubic structure with small amount of hexagonal structure.

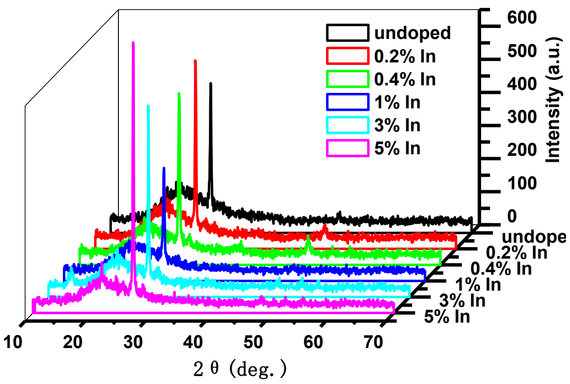

Fig. 1. XRD spectra of CdS films with different indium concentration.

Fig. 2 gives the average grain size of CdS:In films calculated from (111) peak by Debye-Scherrer formula. It can be seen that the relationship between the average grain size and atomic concentration of indium is complex and it suggests that 0.2% and 1% are two critical values for indium atomic concentration. The reason will be discussed in section 2.2 combined with figure 5.

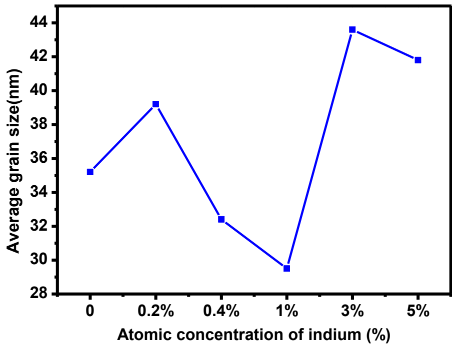

Fig. 2. The grain sizes of CdS films with different indium concentration.

3.2. Optical property of CdS: In films

The transmittance spectra of CdS:In thin films were measured to study the effect of indium on optical property of CdS thin films which is shown in Fig. 3. Fig. 4 shows the zoom in detail of the transmittance in the range of 400nm~600nm. Fig.3 shows that a red shift of the absorption edge happened to all the In-doped films, which is obvious in figure4 from 450 nm to 525 nm. The largest shift appeared in CdS:In films with 0.2% doping concentration. Fig.3 also shows that the average transmittance of indium doped CdS films is slightly lower than that of un-doped CdS film in the range of 550nm~850nm.

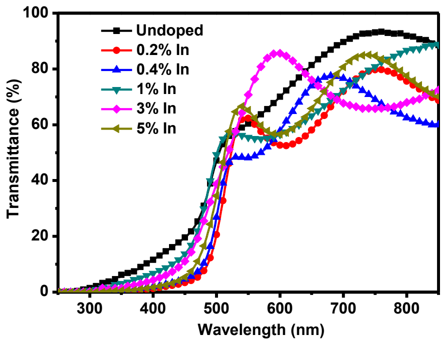

Fig. 3. Transmission of CdS films with different indium concentration.

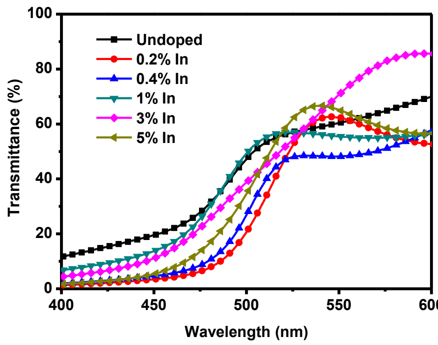

Fig. 4. The zoom in detail of figure 3 (400nm~600nm).

It is well known than CdS thin films are direct band-gap semiconductor materials. The optical energy band gap E_g can be calculated according to Tauc formula:

$$\alpha h\nu = A(h\nu - E_g)^{1/2},$$

where α is the absorption coefficient, h is Planck's constant, A is a constant and E_g is the band gap, respectively. E_g can be obtained through extrapolating $(\alpha h\nu)^2$ vs. photon energy(hν).

The relationship between the energy band gap of CdS:In thin films and the concentration of indium was shown in figure 5. It can be seen that when the indium concentration is about 0.2%, the band gap decrease to a minimum value of 2.42eV while the band gap increase to a maximum(2.51eV) when the indium concentration rise up to 1%. When the indium concentration continues increasing to a higher value (> 1%), the band gap decreases again with the increase of indium concentration. This phenomenon seems strange and difficult to understand. But comparing figure 2 and figure 5, we know that 0.2% and 1% are two critical transition points for these two figures. This phenomenon might be explained as the quantum local effects of nano crystals, which suggests that smaller grain size will lead to larger optical band gap[24].

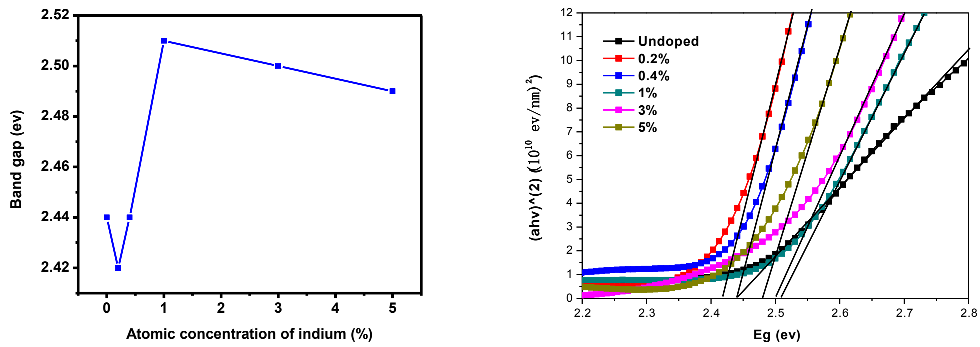

Fig. 5. The band gap of CdS films vs. indium concentration.

3.3. Electrical property of CdS:In films

Table 2 lists the electrical parameters of CdS:In thin films tested by dark Hall measurement. In this measurement, the temperature was set at 300 ± 1K. The thickness of all CdS:In films was 150 nm. According to the Hall effect, the conductivity σ, carrier concentration p and the mobility μ can be described by formula:

$$\sigma_p = pq\mu_p$$

Table 2: Electrical parameters of CdS:In thin films

Doping concentration	Bulk resistivity (/Ω·cm)	Sheet resistance (/Ω□)	Mobility (cm^{-2}/V·Sec)	Carrier concentration(cm^{-3})
0%	16	1.1E+06	/	/
0.2%	10	6.9E+05	1.6	3.7E+17
0.4%	2	1.5E+05	2.4	1.2E+18
1%	0.2	1.1E+04	2.7	1.4E+19
3%	0.4	2.74+04	0.6	2.8E+19
5%	0.1	6.7E+03	1.1	5.6E+19

Table 2 gives the electrical parameters of CdS:In films. However, the Hall measurement for CdS film without doping could not provide mobility and carrier concentration due to the high resistivity of film. From the data in table 2, we can clearly see the remarkable doping effect of indium in CdS films. The carrier concentration increases and the bulk resistivity decreases with indium concentration by 1~3 magnitudes. This is attributed to the increase of extra electrons coming from the In^{3+} ion which replaced the Cd^{2+} sites and reduced the potential barrier of CdS grain boundary. The mobility of electrons in CdS:In films increases from 1.6 $cm^{-2}/V{\cdot}Sec$ to 2.7 $cm^{-2}/V{\cdot}Sec$ when the indium concentration in CdS films is less than 1%. This can be explained as the reduced potential barrier of grain boundary with small amount of indium[25]. However, higher concentration(>1%) of indium leads to lower mobility of electrons, which may be caused by the formation of the secondary phase in the films. Dhere et al. [26] reported that heavily In-doped CdS films prepared by a hot wall technique formed the $CdIn_2S_4$ compound at the grain boundary. Kim et al. [27] considered that the solubility limit of indium in CdS is 3×10^{20} cm^{-3} and the excess indium could form the secondary phase, which is possibly segregated at grain boundaries. The increase of the secondary phase with the increase of In concentration can decrease the carrier concentration and Hall mobility.

Considering the above properties of CdS:In films, we decided to use CdS:In with 0.2% and 0.4% indium as window layer of CdTe solar cells because they have optimal resistivity and optical transmittance while the indium concentration is relatively low, which would not form the secondary phase and add considerable cost to CdTe solar cells.

3.4. CdS:In/CdS/CdTe solar cells

The previous report suggests that CdS:In will form an inferior junction with CdTe film[28], so we designed CdS:In(30 nm)/CdS(20 nm) complex window layer to prevent much indium diffusion into CdTe to degrade p-n junction. FTO substrates were experienced mechanical polishing process to reduce the surface roughness because smooth interface is also a key point to form a good junction with very thin CdS film. AFM measurement shows that the average roughness of polished FTO substrates is about 3 nm. A device structure of FTO/CdS:In/CdS/CdTe/ZnTe:Cu/Au is designed and this kind of solar cells were fabricated. CdTe solar cells with 50nm CdS window layer were used as baseline cells to illustrate the role of indium.

Fig. 6 shows the light *I-V* box chart of CdTe solar cells with three different CdS window layers. The average light *I-V* parameters of CdTe solar cells are shown in table 3. From figure 6, we know that both V_{oc} and J_{sc} increased a little when CdS film was doped with indium, which suggests that indium doping is beneficial to enhance the built-in electrical field between CdS and CdTe films. However, the fill factor of In-doped devices decreased obviously. From table 3, it can be seen that there is big drop of R_{sh} for indium doped devices compared with devices without indium while R_s has not too much difference for three types of devices. So we inferred that introduction of indium might increase the interface density between CdS and CdTe and increase the dark saturation current density of the junction which leads to the obvious decrease of fill factor.

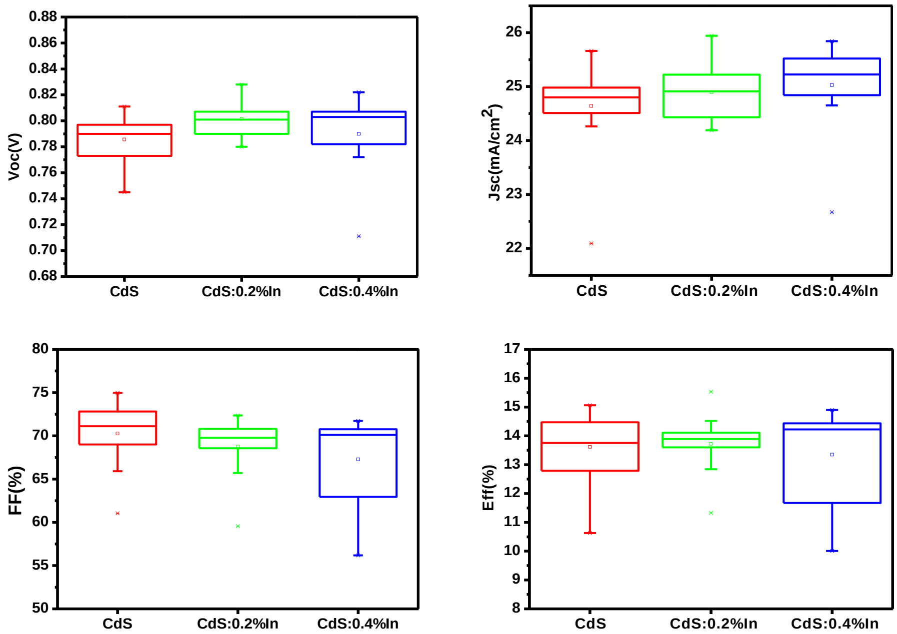

Fig. 6. Box chart of photovoltaic parameters of CdTe solar cells with three different window layers.

Table 3 Average light I-V parameters of CdTe solar cells with different window layers[a]

In concentration in window layer (%)	PCE(%) (average)	V_{oc}(V) (average)	J_{sc}(mA/cm^2) (average)	FF(%) (average)	R_{sh}($\Omega \cdot cm^2$) (average)	R_s($\Omega \cdot cm^2$) (average)
0	13.62	0.785	24.64	70.27	687	3.7
0.2	13.72	0.801	24.90	68.75	807	4.3
0.4	13.35	0.790	25.03	67.28	689	4.3

[a]Based on more than 14 devices for each category.

Fig. 7 shows the EQE of CdTe solar cells with three different CdS window layers. We can clearly see improvements of EQE for devices with indium doped CdS in the range of 350~810nm (especially in 350~500nm) and in other area they are exactly same. This improvement has a dependency with indium concentration and it is more with increasing indium. Combined with the data in table 3, we analyzed that indium doped CdS will enhance the built-in electrical field and then form a p-n junction with improved V_{oc} and J_{sc}. It is noteworthy that the improvement in the range of 350~500nm is more. This suggests a better collection and separation of carriers for indium doped CdS films. When indium was introduced, the carrier concentration of CdS increased and the depletion area extended more deep in CdS layer so as to enhance the EQE from 350nm to 500nm.

The phtoto current density-voltage curves of the best CdTe solar cells for each type of window layer are shown in Fig. 8. A best PCE of 15.53% was obtained in CdS:In(0.2%)/CdTe solar cell with Voc of 0.828V, Jsc of 25.94 mA/cm^2 and FF of 72.36%.

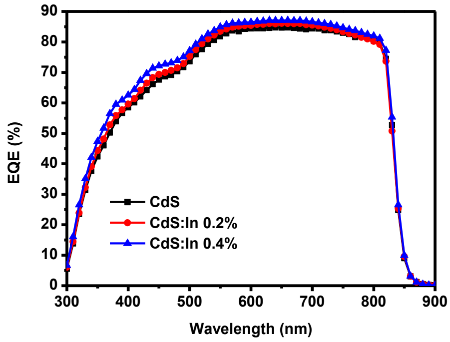

Fig. 7. EQE spectra of CdTe solar cells with three different window layers

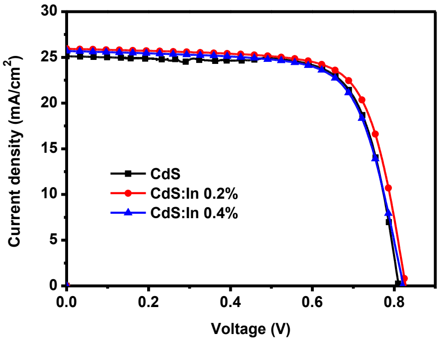

Fig. 8. Best photo current density –voltage characteristics of CdTe solar cells for each window layer

4. Conclusions

The CdS:In films were deposited on glass substrates by magnetron co-sputtered method. The as-deposited CdS:In films were polycrystalline with cubic and hexagonal structure. The (111) direction in cubic structure was observed as a preferential orientation. 0.2% indium concentration was found to be an interesting value due to its lager grain size, narrower band gap. Indium has significant effect on electrical property of CdS film. With the increase of indium doping, the resistivity was decreased from 16Ω·cm to 0.1Ω·cm and the carrier concentration increased to 5.6 $\times 10^{19}$cm^{3}. Indium doped CdS will enhance the built-in electrical field and form a p-n junction with improved V_{oc} and J_{sc}. Up to 15.53% of PCE has been achieved in CdS:In(0.2%)/CdTe solar cells. Indium doped CdS can effectively enhance n type of CdS and built-in electrical field of CdS/CdTe junction, which suggests that indium doping is a simple method with strong potential to further improve the efficiency of CdTe solar cells.

Acknowledgments

This work was financially supported by National High Technology Research and Development Program of China (Grant No.2015AA050610).

References

[1] B. Su, K. L. Choy, Thin Solid Films, **s 361–362**, 102 (2000).

[2] A. G. Valyomana, K. P. Vijayakumar, C. Purushothaman, J. Mater. Sci. Lett. **11**, 616 (1992).

[3] H. Chavez, M. Jordan, J.C. Mcclure, G. Lush, V.P. Singh, J. Mater. Sci. - Mater. Electron. **8**, 151 (1997).

[4] N.A. Shah, R.R. Sagar, W. Mahmood, W.A.A. Syed, J. Alloys Compd., **512**, 185 (2012).

[5] E. Moons, D. Gal, J. Beier, G. Hodes, D. Cahen, L. Kronik, L. Burnstein, B. Mishori, Y. Shapira, D. Hariskos, Sol. Energy Mater. Sol. Cells, **43**, 73 (2013).

[6] M. A. Osman, W.A. Elsaid, A.A. Othman, A.G. Abdelrahim, M.A. Osman, W.A. Elsaid, A. A. Othman, A.G. Abdelrahim, J. Phys. D: Appl. Phys. **49**, 165302 (2016).

[7] S. Mathew, P.S. Mukerjee, K.P. Vijayakumar, Thin Solid Films, **254**, 278 (1995).

[8] T. Sivaraman, V.S. Nagarethinam, A.R. Balu, K. Usharani, J. Mater. Sci. - Mater. Electron. **27**, 1158 (2016).

[9] A. Ashour, N. El-Kadry, S.A. Mahmoud, Thin Solid Films, **269**, 117 (1995).

[10] Dmitri Routkevitch, Terry Bigioni, Martin Moskovits, M.X. Jing, J. Phys. Chem., **23**, 1519 (1996).

[11] J.H. Al-Zahrani, M. El-Hagary, A. El-Taher, Mater. Sci. Semicond. Process., **39**, 74 (2015).

[12] M.A. Hannan, M. Basharat, N.A. Shah, A. Ali, M. Arif, A. Maqsood, Mater. Lett. **62**, 1400 (2008).

[13] C.T. Tsai, D.S. Chuu, G.L. Chen, S.L. Yang, J. Appl. Phys., **79**, 9105 (1996).

[14] S. Hemathangam, G. Thanapathy, S. Muthukumaran, J. Mater. Sci. - Mater. Electron., 1-9 (2016).

[15] J. Avilaavendano, I. Mejia, H.N. Alshareef, Z. Guo, C. Young, M. Quevedolopez, J. Avilaavendano, I. Mejia, H.N. Alshareef, Z. Guo, Thin Solid Films, **608**, 1 (2016).

[16] R. Yang, D. Wang, L. Wan, D. Wang, RSC Adv., **4**, 22162 (2014).

[17] D. Acosta, Sol. Energy Mater. Sol. Cells, **82**, 11 (2004).

[18] B.N. Patil, D.B. Naik, V.S. Shrivastava, Chalcogenide Letters, **8**, 117 (2011).

[19] H. Khallaf, G. Chai, O. Lupan, L. Chow, S. Park, A. Schulte, Appl. Surf. Sci. **255**, 4129 (2009).

[20] J.-H. Lee, J.-S. Yi, K.-J. Yang, J.-H. Park, R.-D. Oh, Thin Solid Films, **431-432**, 344 (2003).

[21] M.A. Islam, K.S. Rahman, F. Haque, N. Dhar, M. Salim, M. Akhtaruzzaman, K. Sopian, N. Amin, F. Haque, N. Dhar, Journal of Ovonic Research, **10**, 185 (2014).

[22] S. Butt, N.A. Shah, A. Nazir, Z. Ali, A. Maqsood, J. Alloys Compd., **587**, 582 (2014).

[23] F. Atay, V. Bilgin, I. Akyuz, S. Kose, Mater. Sci. Semicond. Process., **6**, 197 (2003).

[24] V.I. Klimov, S.A. Ivanov, J. Nanda, M. Achermann, I. Bezel, J.A. McGuire, A. Piryatinski, Nature, **447**, 441 (2007).

[25] M.V. Garcia-Cuenca, J.L. Morenza, J. Esteve, J. Appl. Phys., **56**, 1738 (1984).

[26] N. G. Dhere, H. R. Moutinho, R. G. Dhere, J. Vac. Sci. Technol. A-Vac. Surf. Films, **5**, 1956 (1987).

[27] S.Y. Kim, D.S. Kim, B.T. Ahn, H.B. Im, Thin Solid Films, **229**, 227 (1993).

[28] C.S. Ferekides, D.L. Morel, Process Development for High Voc CdTe Solar Cells, in, University of South Florida, ResearchGate, 2016.